Nonzero ionic size and charge-correlation forces between fluid membranes

Yang Li and Bae-Yeun Ha*
Department of Physics, University of Waterloo, Waterloo, Ontario, Canada N2L 3G1
(Received 14 May 2004; revised manuscript received 30 July 2004; published 3 December 2004)

We present a theoretical approach to charge-correlation attractions between like-charged membranes with neutralizing counterions assumed to be localized to the membrane surface. In particular, we study the effect of nonzero ionic sizes on the attraction by treating the membrane charges (both backbone charges and localized counterions) as forming a two-dimensional ionic fluid of hard spheres of the same diameter D. Using a two-dimensional Debye-Hückel approach to this system, we examine how ion sizes influence the attraction. We find that the attraction gets stronger as surface charge densities or counterion valency increase, consistent with long-standing observations. Our results also indicate a nontrivial dependence of the attraction on separations h: The attraction is enhanced by ion sizes for intermediate h ranges, while it crosses over to the known D-independent universal behavior as $h \to \infty$; it remains finite as $h \to 0$, as expected for a system of finite-sized ions.

DOI: 10.1103/PhysRevE.70.061503 PACS number(s): 61.20.Qg, 82.70.−y, 87.15.Ya

I. INTRODUCTION

Counterion-induced attractions between like charges are ubiquitous in biology, as a large class of biological processes rely on these attractions [1–5]. Some viruses use multivalent counterions in their host cells to package their DNA, which carries a negative charge in aqueous solution [1,2]. These attractions are also responsible for the formation of bundles of other kinds of stiff polyelectrolytes such as microtubules and actin filaments [3], which are crucial to the mechanical properties of living cells. Membrane adhesion can also be promoted by multivalent counterions such as Mg^{2+} and Ca^{2+} [6].

Since the mean-field approach of Poisson-Boltzmann theory always predicts repulsion between like charges, the electrostatic mechanism behind these observations has been a subject of intensive research in the past few decades, producing a number of seemingly distinct theoretical approaches [7–19]. In all these approaches, the attraction arises from correlations between counterions, especially those in the close proximity of their coions. The major difference between them lies in the way they capture ion correlations. For example, an integral-equation method has been used to account for counterion-density correlations [8,9]. This approach relies on an approximation scheme, namely, a closure for pair correlation functions, and often requires heavy numerical analysis. In more analytical treatment [12,17], charge fluctuations are captured at the Gaussian level. For unscreened planar cases (e.g., charged bilayers in a low-salt limit), the electrostatic pressure shows universal power-law behavior at large separations [9,10,12]: $\Pi(h/\lambda \to \infty) \equiv \Pi_\infty \sim -k_B T/h^3$, where h is the separation, k_B is the Boltzmann constant, and T is the temperature. Finally λ is the Gouy-Chapmann length, a length scale within which most counterions are localized [see the more precise definition of λ below Eq. (2)]. This result is independent of surface charge densities and counterion valency. In a low-temperature picture [16], the attraction is reminiscent of a strong charge correlation that drives the system into an ionic crystal at zero temperature and decays exponentially with h. There are some variations of this approach [18,19], but they do not deviate in spirit significantly from it. More recently, it has been shown that a more complete theory should incorporate both kinds of behavior [20,21]: the power-law pressure and the exponential pressure. Depending on surface charge densities or temperature, the short-ranged, exponentially decaying pressure can be dominant at short separations, but it should cross over to the power-law pressure as h increases. Finally, strong-coupling (SC) theory has been proposed that becomes asymptotically exact in the strong-coupling limit (i.e., low temperatures, high surface charge densities, and large counterion valency) [22,23].

Despite all this effort, the problem of counterion-induced attraction still remains challenging. Many existing (analytically tractable) theoretical approaches [4,7,9,11–19] rely on a common approximation for charges: point charges. While some aspects of nonzero ionic sizes were discussed in a more numerical treatment in the literature (see, for example, Ref. [9]), a more comprehensive picture is highly sought after. It is also desirable to develop a more analytical approach that will provide a more direct picture of how finite ionic sizes influence the electrostatic attraction. The main purpose of this paper is to discuss the effects of ionic sizes on the electrostatic attraction between like-charged surfaces. Here we do not attempt to further reconcile the discrepancy between existing approaches. Instead we will develop two-dimensional Debye-Hückel (DH) theory (i.e., linearized Poisson-Boltzmann theory) for highly charged surfaces with neutralizing counterions assumed to be localized to the surface—delocalized counterions will not be taken into account. Here, both backbone charges and counterions are modeled by hard spheres of the same diameter D as in the restrict primitive model [27]. The main advantage of our approach lies in that it provides a simple physical picture for the attraction without being complicated by other competing effects. We find that the effect of finite D is dramatic: In

*Corresponding author.

 ©2004 The American Physical Society

contrast to Π_∞, which is independent of σ (planar charge densities) or Z (counterion valency), the DH pressure for $D>0$ can be sensitive to σ and gets stronger as σ or Z increases in magnitude (unless h is too small). This is intriguing as it indicates that ionic sizes influence the σ (or Z) dependence of the pressure. Our results are consistent with long-standing observations of stronger attractions for higher σ_0 or larger Z [9,16,24,25]. Our results also indicate nontrivial dependence of the attraction on h. While the attraction reduces to the limiting pressure Π_∞ in the limit $h\to\infty$, it shows D dependence for h ranges of physical interest. The attraction is enhanced by ionic sizes for moderately large h ($h\gtrsim 5$ Å), but it approaches a finite value as $h\to 0$. The ionic size enhances a charge polarity, leading to a stronger attraction unless h is too small. On the other hand, the free energy (per area) for $D>0$ is finite, leading to a finite attraction (per area) as $h\to 0$. However, our approach may leave out strong coupling between ions that becomes important at low temperatures and can be considered as complementary to SC theory [22,23].

II. MODEL AND INTERACTION FREE ENERGY

To be specific, we consider two parallel surfaces perpendicular to the z axis, a distance h apart. Each surface is assumed to be negatively charged with the same backbone charge density $\sigma\equiv -e\sigma_0$, with $-e$ the electronic charge. For sufficiently large σ_0 (>0), the Gouy-Chapman length λ, a length scale beyond which each surface is neutralized, is smaller than typical ion sizes. In this case, it is useful to classify counterions into two subclasses [4,7]: "condensed" and "free." In this simplified picture, both backbone charges and condensed counterions are approximated to lie in the same plane of the surface—they give rise to in-plane charge fluctuations that become correlated from one surface to the other, leading to an attraction. For simplicity, we will not include free (delocalized) counterions. Here, we adopt the so called restricted primitive model [26,27] of ions and treat both backbone charges and condensed counterions as hard spheres of the same diameter D, carrying charge at the center. As a result, the interaction between two charges q and q' separated by a distance r assumes the following form [27]:

$$U(r)=\begin{cases}\infty, & r<D,\\ \dfrac{qq'}{\epsilon r}, & r>D.\end{cases} \tag{1}$$

Here the dielectric constant ϵ is assumed to be constant throughout the system (thus suppressing dielectric discontinuity) and will be taken to be that of water. Furthermore, we assume that condensed counterions have the same valency Z. This is reasonable, since multivalent counterions are preferentially adsorbed onto a highly charged surface [28].

In order to treat condensed counterions and backbone charges on equal footing, we use $Z_\alpha e$ to denote the charge on the two different kinds of ions: $Z_\alpha=Z$ for counterions and $Z_\alpha=-1$ for backbone charges. The overall electric neutrality then requires $\Sigma_\alpha Z_\alpha\sigma_\alpha=0$ [29] (note that $Z_\alpha e\sigma_\alpha$ is the surface charge density of the αth kind of ions). Most of the crucial properties of the resulting system can be studied by holding an ion on one of the surfaces and examining how other ions respond to it [26,27]. To this end we put an ion of charge Z_α at the origin on surface 1, and calculate the electric potential created by this ion and the surrounding ionic cloud of opposite charge, denoted by $\Psi_j(\mathbf{r})$, where j (=1,2) runs over surfaces at $z=0$ and h, respectively. In Debye-Hückel theory, the electrostatic potential at position $\mathbf{r}$ is then described by the following differential equation (see Ref. [27] for a three-dimensional analog):

$$\nabla^2\Psi(\mathbf{r})=\begin{cases}-\dfrac{4\pi}{\epsilon}Z_\alpha e\,\delta(\mathbf{r}), & r<D,\\ \dfrac{2}{\lambda}\Psi(\mathbf{r})[\delta(z)+\delta(z-h)], & r>D,\end{cases} \tag{2}$$

where $\lambda^{-1}=2\pi\ell_B\Sigma_\alpha Z_\alpha^2\sigma_\alpha$. The validity of this approach can be checked *a posteriori*—see the relevant discussion below Fig. 4. The overall neutrality requires $\lambda^{-1}=2\pi\ell_B(Z+1)\sigma_0$. Here we are particularly interested in the electric potential in the plane of the surface: $\psi_1(\mathbf{r}_\perp)\equiv\Psi(\mathbf{r}_\perp,z=0)$ and $\psi_2(\mathbf{r}_\perp)=\Psi(\mathbf{r}_\perp,z=h)$, where $\mathbf{r}_\perp=(x,y)$. We find, for $r>D$,

$$\psi_1(\mathbf{r}_\perp)=Av_{11}-\frac{\lambda^{-1}}{2\pi}\int d\mathbf{r}'_\perp\sum_{j=1}^{2}\psi_j(\mathbf{r}'_\perp)v_{1j}(\mathbf{r}'_\perp-\mathbf{r}_\perp),$$

$$\psi_2(\mathbf{r}_\perp)=Av_{12}-\frac{\lambda^{-1}}{2\pi}\int d\mathbf{r}'_\perp\sum_{j=1}^{2}\psi_j(\mathbf{r}'_\perp)v_{2j}(\mathbf{r}'_\perp-\mathbf{r}_\perp), \tag{3}$$

where $v_{ij}=1/\sqrt{r_\perp^2+h_{ij}^2}$ and $h_{ij}=h$ if $i\neq j$ and 0 otherwise. Note here that the integration constant A is not automatically set in the two-dimensional case, in contrast to the corresponding three-dimensional case where it is fixed by Gauss' law [26]. It proves useful to introduce a matix M defined by matrix elements

$$M_{ij}(\mathbf{k}_\perp)=\delta_{ij}+\frac{e^{-h_{ij}k_\perp}}{\lambda k_\perp}. \tag{4}$$

In terms of this, $\psi_1(\mathbf{r}_\perp)$ and $\psi_2(\mathbf{r}_\perp)$ are given as follows:

$$\psi_1(\mathbf{r}_\perp)=A\lambda\int k_\perp dk_\perp \times\frac{M_{11}(\mathbf{k}_\perp)[M_{11}(\mathbf{k}_\perp)-1]-M_{12}^2(\mathbf{k}_\perp)}{\det[M(\mathbf{k}_\perp)]}J_0(k_\perp r_\perp),$$

$$\psi_2(\mathbf{r}_\perp)=A\lambda\int k_\perp dk_\perp\frac{M_{12}(\mathbf{k}_\perp)}{\det[M(\mathbf{k}_\perp)]}J_0(k_\perp r_\perp), \tag{5}$$

where $J_0(x)$ is the zeroth-kind Bessel function of the first kind. The constant A can be determined by imposing the electric neutrality condition

$$Z_\alpha e=\frac{\epsilon}{\lambda}\left(\int_D^\infty dr_\perp r_\perp\psi_1(r_\perp)+\int_0^\infty dr_\perp r_\perp\psi_2(r_\perp)\right). \tag{6}$$

Note that the region $r_\perp<D$ is included in the second integral.

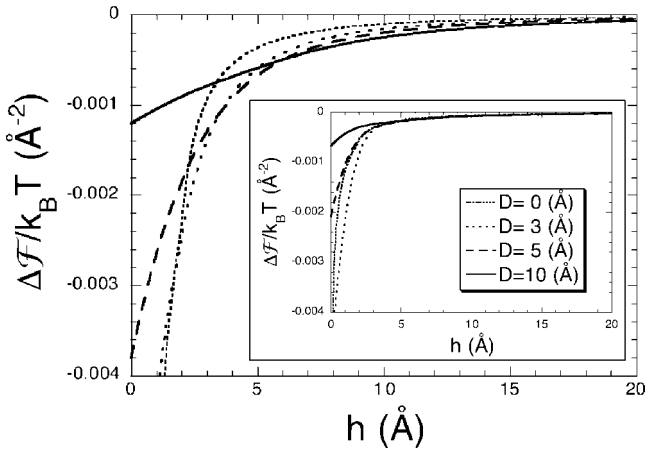

FIG. 1. The electrostatic free energy of each plate per unit area, $\Delta\mathcal{F}$, as a function of separation h for various choices of D. We have chosen $T=300$ K, $\epsilon=80$, and $\lambda=1$ Å. For $h\gtrsim 5$ Å, the free energy gets more negative as the ion size D increases. For $\lambda=5$ Å (see the inset), however, $\Delta\mathcal{F}$ is less sensitive to D as long as $h\gtrsim 5$ Å. As $h\to 0$, however, $\Delta\mathcal{F}$ in both cases remains finite as long as $D>0$ and is less attractive for larger D.

Following the Debye charging process [26,27], the charge fluctuation contribution to the free energy can be obtained. If we consider ψ_1 as a function of $r_\perp$ and e, i.e., $\psi_1(r_\perp,e)$, then the electrostatic free energy of each plate per unit area is given as the following integral:

$$\frac{\mathcal{F}}{k_BT}=\frac{1}{2\pi}\left(\frac{\epsilon}{\lambda Z_\alpha e}\int_0^1\frac{d\zeta}{\zeta}\psi_1(D,\zeta e)-\frac{1}{2D\lambda}\right). \tag{7}$$

Note that ψ_1 incorporates both interplate and in-plane charge correlations and is h dependent. The free energy in Eq. (7) enables us to systematically study the effect of ionic sizes on the electrostatic attraction between the two plates. As $D\to 0$, this approach reproduces the known result of Ref. [12].

To study the effect of ionic sizes, we have computed the free energy per unit area with reference to $h=\infty$: $\Delta\mathcal{F}=\mathcal{F}(h)-\mathcal{F}(h=\infty)$. Figure 1 shows $\Delta\mathcal{F}$ (in units of k_BT) as a function of the separation h for different values of the diameter D. We have chosen the parameters $T=300$ K, $\epsilon=80$ (hence $\ell_B=7.1$ Å), and $\lambda=1$ Å (typical value for DNA or fully charged bilayers). Ionic sizes have nontrivial effects on $\Delta\mathcal{F}$: For $h\gtrsim 5$, $\Delta\mathcal{F}$ gets more negative as D increases. A plausible reason for this is that larger D results in a larger charge polarity—the charge distribution is more heterogeneous—and hence an enhanced attraction. To understand this more clearly, consider a backbone charge on one of the plates (assumed to be at the origin) and its ionic cloud of thickness $\sim\lambda$. Beyond the length scale $\sim D+\lambda$, this plate will appear to be overall neutral to charges on the other plate. Accordingly, this charge (surrounded by the ionic cloud) can be more sensitively felt by counterions on the other plate if D is larger. This may account for the stronger attraction between the plates for larger D. (Similar arguments based on a zero-temperature picture can be found in Ref. [16].)

On the other hand, for smaller h, larger D implies a weaker attraction. At first glance, this is somewhat puzzling. As it turns out, the small-h behavior reflects single-plate properties. As $h\to 0$, the two-plate system resembles a single plate with a surface charge density twice that of each plate: $\Delta\mathcal{F}(\sigma,h\approx 0)\approx\mathcal{F}_1(2\sigma)/2-\mathcal{F}_1(\sigma)$, where $\mathcal{F}_1(\sigma)\equiv\mathcal{F}(\sigma,h=\infty)$ is the corresponding free energy of each plate [26]. For point charges, $\mathcal{F}_1$ diverges (opposite charges can get arbitrarily close to each other). We find that, for $D\ll\lambda$, $\lim_{h\to 0}\Delta\mathcal{F}\to-(k_BT/4\pi\lambda^2)\log(\lambda/D)$. For $D\gg\lambda$, however, $\lim_{h\to 0}\Delta\mathcal{F}(h)\to-(k_BT/4\pi D^2)\log(D/\lambda)$. This analysis implies that $|\Delta\mathcal{F}(h\approx 0)|$ decreases as D increases and remains finite as long as $D>0$, consistent with our results in Fig. 1.

For the more weakly charged case of $\lambda=5$ Å (see the inset), however, $\Delta\mathcal{F}$ is almost insensitive to D for large h, i.e., $h\gtrsim 5$ Å. On the other hand, for $h\lesssim 5$ Å, the effect of nonzero D becomes more pronounced: $|\Delta\mathcal{F}(h<5\ \text{Å};D>0)|$ is smaller for larger D, as in the case of $\lambda=1$ Å.

To study the h dependence of the free energy (per area plate), i.e., $\Delta\mathcal{F}$, we have displayed $|\Delta\mathcal{F}|$ in units of k_BT as a function of h in a log-log plot, for two different choices of D (see Fig. 2): $D=0$ (dashed line) and $D=5$ Å (circles). We have chosen $T=300$ K and $\epsilon=80$. Figures 2(a) and 2(b) correspond to $\lambda=1$ and 5 Å, respectively. First consider the case $\lambda=1$ Å in (a). In this case, the free energy for $D=0$, $\Delta\mathcal{F}_0\equiv\Delta\mathcal{F}(D=0)$, essentially follows the universal scaling behavior $\Delta\mathcal{F}_\infty\sim-1/h^2$—the $D=0$ curve is essentially a straight line with a slope of about 2 throughout the entire range of the plot ($h\gtrsim 5$ Å). On the other hand, the h dependence of $\Delta\mathcal{F}$ for $D=5$ Å is more complicated. The free energy is no longer a straight line in the log-log plot, indicating the existence of multiple scaling regimes. To analyze this case, we plot the difference $\delta\Delta\mathcal{F}\equiv\Delta\mathcal{F}(D=5\ \text{Å})-\Delta\mathcal{F}_0$ (triangles). The $1/h^2$ dependence has been subtracted and the resulting $\delta\Delta\mathcal{F}$ should reflect ion sizes (and charge densities)—$\delta\Delta\mathcal{F}$ depends on D (and λ). The slope of this curve s becomes steeper as h increases and thus does not assume a simple scaling form. It, however, eventually becomes a constant $s\approx 2.9$ as $h\to 1000$ Å. This implies that, for large h, $\Delta\mathcal{F}\sim\Delta\mathcal{F}_\infty+a_3/h^s$, where a_3 is the coefficient of the $1/h^s$ term. This large-h behavior is consistent with Ref. [9] in which it was shown that $\Pi-\Pi_\infty\sim-A_4/h^4$ in the limit of $h\to\infty$, where λ and D dependence is implicitly included through the coefficient A_4. In this expansion or our free energy expansion, the term depending on D (and λ) decays faster than $\Delta\mathcal{F}_\infty$. To understand this, first recall that long-wavelength fluctuations lead to a long-ranged interaction; if $\Delta\mathcal{F}_\infty$ arises from $k_\perp\simeq 0$, then higher-order terms come from higher $k_\perp$. In light of this, it is not surprising that $\Delta\mathcal{F}_\infty$ does not reflect λ or D dependence, which should be washed out at large-length scales (see also Ref. [9]). A straight line tangent to this curve at large h ($h=1000$ Å) intersects the $D=0$ curve at $h=h_{cr}\approx 40$ Å. This implies that the crossover from $1/h^2$ to $1/h^s$ takes place at $h=h_{cr}$. For $h<h_{cr}$, the free energy decays as $1/h^s$. Beyond this separation, however, it is dominated by $\Delta\mathcal{F}_\infty$.

Figure 2(b) shows the corresponding results for $\lambda=5$ Å. First note that, for $h\gg 5$ Å, the $D=0$ curve ($\Delta\mathcal{F}_0$) is essentially the same as in the case $\lambda=1$ Å; $\Delta\mathcal{F}_0$ for $h\gg\lambda$ follows a universal scaling law [9,12]. The main difference between the cases ($\lambda=5$ and 1 Å) is through the D-dependent term

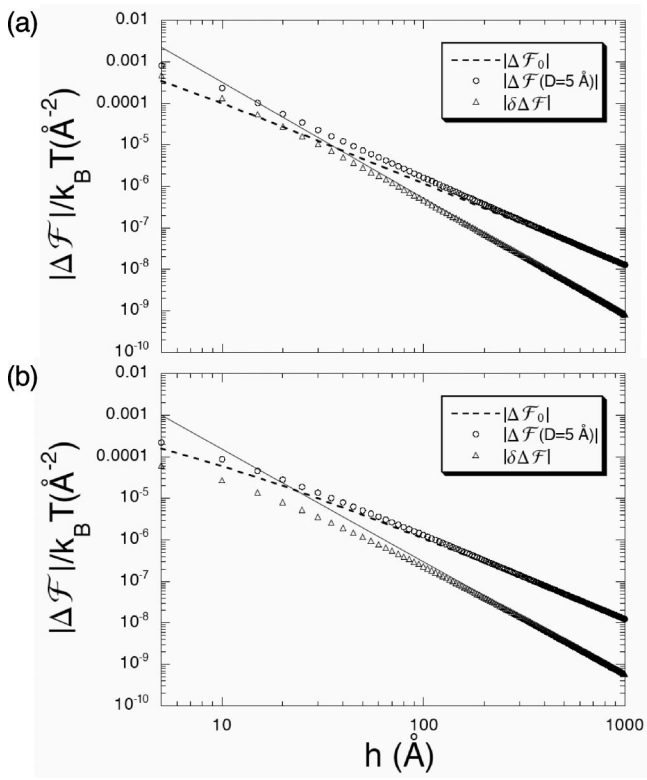

FIG. 2. Log-log plot of $\Delta\mathcal{F}$, i.e., the electrostatic free energy of each plate per unit area as a function of separation h, for (a) $\lambda=1$ Å and (b) $\lambda=5$ Å. We have chosen $T=300$ K and $\epsilon=80$. (a) The free energy curve for $D=0$ ($\Delta\mathcal{F}_0$) is a straight line with a slope 2, confirming the known universal result: $\Delta\mathcal{F}_\infty\sim -k_BT/h^2$. The free energy curve for $D=5$ Å is no longer a straight line, indicating the existence of multiple scaling regimes: The slope of $\delta\Delta\mathcal{F}\equiv\Delta\mathcal{F}(D=5\ \text{Å})-\Delta\mathcal{F}_0$ approaches $s\approx 2.9$ as $h\to\infty$. Our analysis suggests that the free energy is dominated by $\delta\Delta\mathcal{F}\sim 1/h^s$ for $h\lesssim h_{cr}\approx 40$ Å and crosses over to $\Delta\mathcal{F}_\infty$ at $h\approx h_{cr}$. (b) For a larger $\lambda=5$ Å, the crossover takes place at a smaller value of h: $h_{cr}\approx 20$ Å. Note that the free energy for $D=0$ in this case is essentially the same as in the previous case (a) for $h\gg\lambda$, as expected.

$\delta\Delta\mathcal{F}\sim 1/h^s$ and is twofold: For the larger λ, the free energy is less negative and the crossover takes place at a smaller separation ($h_{cr}\approx 20$ Å). Consequently, the effect of nonzero ionic sizes becomes more pronounced for a more highly charged surface—the prefactor of $\delta\Delta\mathcal{F}$ is larger in magnitude for smaller λ.

In light of our results in Fig. 2, we have carried out an asymptotic analysis of the free energy $\Delta\mathcal{F}$ (per plate area). In this limit $h\gg D\gg\lambda$, we find (in the Appendix)

$$\frac{\Delta\mathcal{F}}{k_BT}\sim -\frac{\zeta(3)}{32\pi}\left[\frac{1}{h^2}+\frac{D}{h^3}\ln\frac{h}{\lambda}\right], \tag{8}$$

where $\zeta(n)$ is the Riemann zeta function with $\zeta(3)\approx 1.202$. The first term is the universal power law $\Delta\mathcal{F}_\infty$. On the other hand, the second term arises from finite ionic sizes and makes the free energy more negative. Strictly speaking, this result is valid in the limit $h\gg D\gg\lambda$. Nevertheless, this illustrates the significance of finite ionic sizes: The main effect of finite ionic sizes is to make charge distributions more heterogeneous, leading to a larger charge polarity (hence a stronger attraction). It is worth comparing this with the corresponding expansion for $D=0$: $\Delta\mathcal{F}_0\sim -(h^{-2}-2\lambda h^{-3})$. The second term in this equation is distinct from the D-dependent term in Eq. (8). If the former is repulsive, the latter is attractive. Along this line, it should be emphasized that the latter is analogous to $\delta\Delta\mathcal{F}\sim -1/h^s$ in Fig. 2, in the sense that this makes the attraction stronger and is dominant up to h_{cr}, which is larger for larger σ_0. On the other hand, the $1/h^3$ contribution for $D=0$ becomes negligible for highly charged cases. Finally our asymptotic result in Eq. (8), especially the second term, is valid for $h\gg D,\lambda$; $\delta\Delta\mathcal{F}$ approaches this term in this limit. In intermediate regions, the D or λ dependence of $\delta\Delta\mathcal{F}$ can be more complicated than this implies.

In Fig. 3, we present electrostatic pressures (per unit area) Π obtained from a few different approaches: the universal pressure, i.e., $\Pi_\infty\sim -k_BT\zeta(3)/8\pi h^3$ (thin solid line), the DH theory of point charges [12] (dotted lines), our DH approach for $D>0$ (thick solid lines), and the hypernetted chain (HNC) approximations (diamonds) adopted from Fig. 3 of Ref. [9]. Note that essentially the same model was used in the HNC calcualtions: two overall neutral surfaces carrying mobile cations and anions. In our convention $\Pi=-\partial(2\Delta\mathcal{F})/\partial h$. (Recall $\Delta\mathcal{F}$ is the free energy per plate area.) For our calculations, we have chosen the parameters consistent with Ref. [9]: $D=4$ Å, $T=300$ K, $\epsilon=80$ (dielectric discontinuity is suppressed in these cases), (a) $\sigma_0^{-1}=500$ Å^2 and $Z=1$ ($\lambda=5.6$ Å), (b) $\sigma_0^{-1}=200$ Å^2 and $Z=1$ ($\lambda=2.24$ Å, and (c) $\sigma_0^{-1}=75$ Å^2 and $Z=2$ ($\lambda=0.56$ Å). In all these cases, both the HNC results and ours are more attractive than the $D=0$ curves (by several factors at most) for the range shown ($h\geqslant 5$ Å). This clearly suggests that finite ionic sizes enhance the attraction (unless h is too small). For this reason, our results for $D=4$ Å agree better with the HNC results than the $D=0$ curves. The agreement is excellent for $h\gtrsim 5$ Å in (a) and (b). The discrepancy between our and the HNC result for $\sigma_0^{-1}=75$ Å^2 at small separations can be attributed to the appearance of a short-range pressure in the latter, which our DH approach suppressed. But note that, in a bilayer system at room temperature, this high density is realized only when the bilayer is fully charged. As h increases, all these results tend to collapse onto the asymptotic pressure as they should. The results in the figure also show how $D=0$ curves approach the universal pressure Π_∞ as σ_0 increases. Also Π_∞ appears to be favorably compared with both our result and the HNC result for $\sigma_0^{-1}=200$ Å^2. But this is a coincidence; if we chose larger values of D, then both our and the HNC results would predict more attractive pressures, while Π_∞ remains the same.

To further study the consequence of finite ionic sizes, we plot, in Fig. 4, the free energy per unit area $\Delta\mathcal{F}$ (in units of k_BT) as a function of λ. We have chosen $h=10$ Å, $T=300$ K, and $\epsilon=80$. As shown in the figure, $\Delta\mathcal{F}$ is sensitive to λ and is more attractive for small λ (corresponding to high σ_0 or Z). These results are consistent with numerical data [24,25] but deviate from the corresponding results for point charges (the dotted line), which is roughly independent of λ. The results for point charges are somewhat different from the

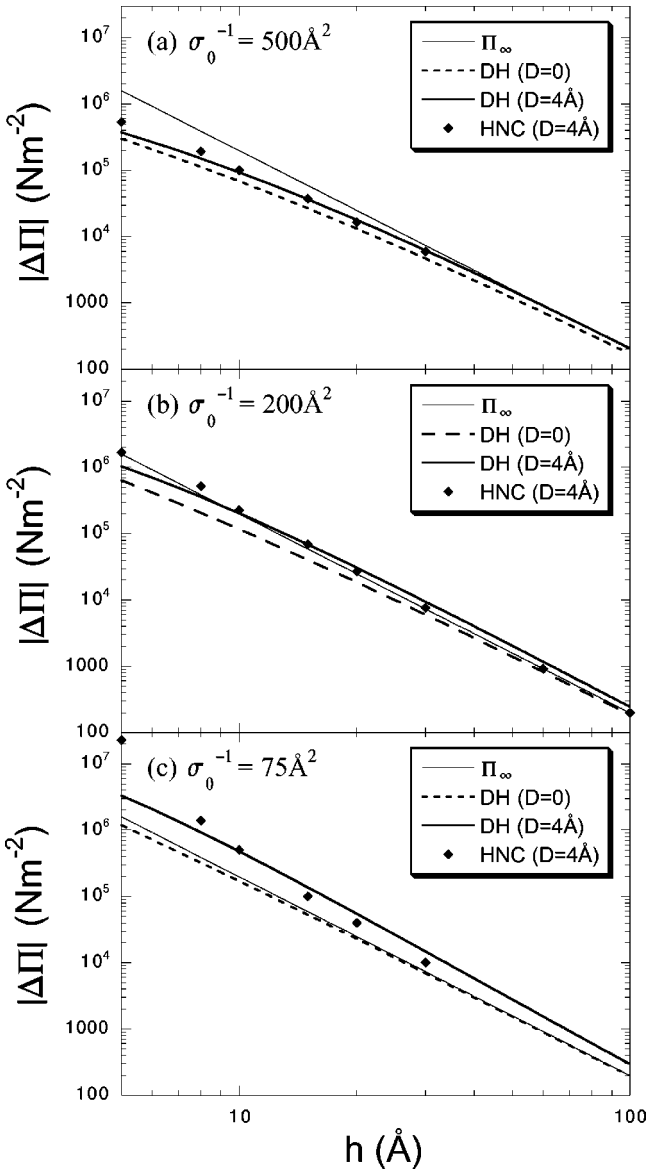

FIG. 3. Log-log plot of the electrostatic pressure Π per unit area as a function of separation h, for (a) σ_0^{-1}=500 Å^2, Z=1, (b) σ_0^{-1} =200 Å^2, Z=1, and (c) σ_0^{-1}=75 Å^2, Z=2. In all cases, T=300 K and ϵ=80. Both our results [DH (D=4 Å)] and the hypernetted chain (HNC) approximations for D=4 Å from Ref. [9] (diamonds) are more attractive than the corresponding DH results for D=0; the effect of nonzero ionic sizes is more pronounced for larger σ_0. As $h\to\infty$, all these results tend to collapse onto the limiting pressure $\Pi_\infty=\Pi(h\to\infty)\sim -k_BT/h^3$. The agreement between the HNC results and ours is excellent except for Π at $h\simeq 5$ Å in (c).

λ-independent $\Delta\mathcal{F}_\infty$; the latter is simply the large-h limit of the former. Note here that the difference between the D=0 pressure and the results for $D\neq 0$ in Fig. 4 solely comes from nonzero ionic sizes, since the two are otherwise identical. This is intriguing since it implies that short-length-scale properties, i.e., ionic sizes, qualitatively modify λ dependence of $\Delta\mathcal{F}$ (unless h/λ is too large). For D=0, the asymptotic limit, characterized by Π_∞, is realized if $h\gg\lambda$. Our results in Fig. 2, however, indicate that for $D>0$ a new length scale comes in: h_{cr}, which is typically much larger

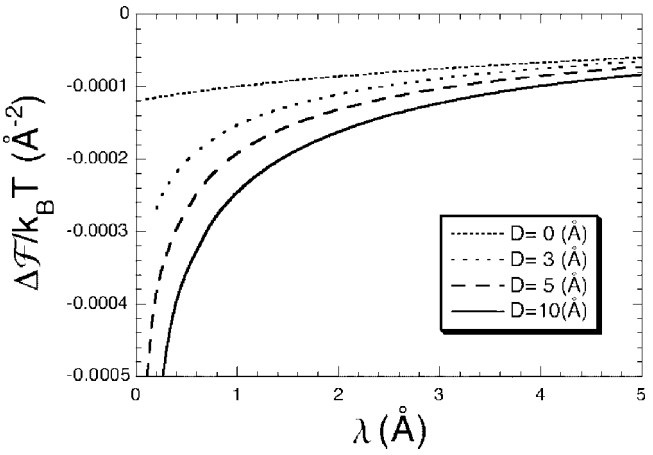

FIG. 4. The electrostatic free energy per unit area (in units of k_BT) as a function of λ. We have chosen h=10 Å, T=300 K, and ϵ=80. As shown in the figure, $\Delta\mathcal{F}$ is sensitive to λ and is more attractive for small λ (corresponding to highly charged case).

than D (see the relevant discussion around Fig. 2). In this case, the asymptotic region is reduced down to $h\gg h_{cr}$. For $h\lesssim h_{cr}$, the electrostatic pressure is sensitive to λ as evidenced in Fig. 4; it is more sensitive to λ and larger in magnitude for larger D (for h=10 Å).

Our DH approach amounts to keeping charge fluctuations at the Gaussian level, leaving out strong charge fluctuations at short length scales as implied by oscillatory charge correlations at low temperatures [20]. In a linearized approach, some of this effect can be, in principle, incorporated by allowing the formation of ion pairs between backbone charges and counterions as much the same way as in the two state model for counterions. The study of the competition between long-wavelength fluctuations and local ordering is a nontrivial one as it depends on separations [20] as well. Moreover, it has been shown that out-of-plane charge fluctuations are important and thus the two-dimensional DH approach inevitably underestimates the negative pressure [13,23]. In addition, it has been shown that surface-charge discreteness can lower the electrostatic pressure Π [14], making it more attractive. Note that this effect arises from enhanced counterion condensation and is distinct from the enhanced attraction (for large D) in our case. In this regard, the spatial distribution of counterions will further complicate Π. Hence further consideration is certainly warranted. Nevertheless our results can be used to check the self-consistency of our DH approach *within* the two-state model of counterions. In the case of physical interest, i.e., $h\gtrsim D\simeq 5$–10 Å, the magnitude of the h-dependent correlation energy is smaller than k_BT. In that case, the DH approach ought to be good. The agreement of our results with those adopted from Ref. [9] is hence not accidental.

III. SUMMARY

In summary, we have developed a theoretical formalism to account for the interplay between ionic sizes and the electrostatic attraction between like charged bilayers. To this end, we have modeled ions (both lipid charges and condensed

counterions) as charged hard spheres of diameter D as in the restricted primitive model of a simple ionic fluid. Using a (two-dimensional) Debye-Hückel approach to this system, we have examined how nonzero ionic sizes are intertwined with the attraction. The nonzero ionic size can qualitatively modify the attraction. In the case of physical interest ($h \gtrsim 5$ Å), it enhances the attraction. A plausible reason for this is that the in-plane charge distribution becomes more heterogeneous as D increases, resulting in a larger charge polarity and hence an enhanced attraction. Also the attraction gets stronger as the surface charge density (in units of $-e$) σ_0 increases, consistent with known results [9,16,24]. This observation is interesting, as it implies that the ionic size influences σ_0 dependence of the attraction. In other words, these two effects (ionic sizes and σ_0 dependence of the attraction) are coupled to each other—the attraction is more sensitive to σ_0 for larger D. Our results are in accord with the long-standing observation of enhanced attractions for high charge densities or large valency and also predicts more realistic results for the pressure that remains finite as $h \to 0$. The main advantage of our approach is that it allows us to systematically study the correlation attraction, without relying on additional approximations/assumptions in addition to linearization that might obscure the essential physics of correlation attractions.

ACKNOWLEDGMENTS

This work was supported by the Natural Science and Engineering Research Council of Canada (NSERC). We thank R. Netz for useful discussions.

APPENDIX

In this appendix, we present an asymptotic result for the free energy (per plate area), $\Delta\mathcal{F}=\mathcal{F}(h)-\mathcal{F}(h=\infty)$, in the limit of $h \gg D \gg \lambda$. To this end, we first write $\psi_1(r_\perp)$ explicitly as an integral with respect to $k_\perp$; if we define

$$\overline{\psi}_1(\mathbf{r}_\perp) = \int k_\perp dk_\perp \frac{M_{11}(\mathbf{k}_\perp)[M_{11}(\mathbf{k}_\perp)-1]-M_{12}^2(\mathbf{k}_\perp)}{\det[M(\mathbf{k}_\perp)]} J_0(k_\perp r_\perp),$$

$$\overline{\psi}_2(\mathbf{r}_\perp) = \int k_\perp dk_\perp \frac{M_{12}(\mathbf{k}_\perp)}{\det[M(\mathbf{k}_\perp)]} J_0(k_\perp r_\perp), \tag{A1}$$

we have

$$\psi_1(\mathbf{r}_\perp) = A\lambda\overline{\psi}_1(\mathbf{r}_\perp),$$

$$\psi_2(\mathbf{r}_\perp) = A\lambda\overline{\psi}_2(\mathbf{r}_\perp). \tag{A2}$$

The constant A, as determined by Eq. (6), is

$$A = \frac{Z_\alpha e}{\epsilon} \frac{1}{\int_D^\infty dr_\perp r_\perp \overline{\psi}_1(r_\perp) + \int_0^\infty dr_\perp r_\perp \overline{\psi}_2(r_\perp)}. \tag{A3}$$

To carry out the r integrals in the denominator, we note that

$$\begin{aligned}\int_D^\infty dr_\perp r_\perp \overline{\psi}_1(r_\perp) + \int_0^\infty dr_\perp r_\perp \overline{\psi}_2(r_\perp) &= -\int_0^D dr_\perp r_\perp \overline{\psi}_1(r_\perp) + \int_0^\infty dr_\perp r_\perp \overline{\psi}_1(r_\perp) \\ &\quad + \int_0^\infty dr_\perp r_\perp \overline{\psi}_2(r_\perp) \\ &= \int_0^\infty dr_\perp r_\perp [\overline{\psi}_1(r_\perp) + \overline{\psi}_2(r_\perp)] - \int_0^D dr_\perp r_\perp \overline{\psi}_1(r_\perp).\end{aligned} \tag{A4}$$

Using this relation [30]

$$\int_0^\infty J_0(k_\perp r_\perp) r_\perp dr_\perp = \frac{\delta(k_\perp)}{k_\perp}, \tag{A5}$$

where $\delta(x)$ is the Dirac δ function, we can simplify the first integral in Eq. (A4) as

$$\begin{aligned}\int_0^\infty dr_\perp r_\perp [\overline{\psi}_1(r_\perp) + \overline{\psi}_2(r_\perp)] &= \int_0^\infty dk_\perp \delta(k_\perp) \left[1 - \frac{1}{M_{11}(\mathbf{k}_\perp) + M_{12}(\mathbf{k}_\perp)}\right] \\ &= 1.\end{aligned} \tag{A6}$$

If we note that

$$\int_0^D dr_\perp r_\perp k_\perp J_0(k_\perp r_\perp) = D J_1(k_\perp D), \tag{A7}$$

where $J_1(x)$ is the first-order Bessel function of the first kind, we can rewrite the second integral in Eq. (A4) as

$$\int_0^D dr_\perp r_\perp \overline{\psi}_1(r_\perp) = D\int_0^\infty dk_\perp \frac{M_{11}(\mathbf{k}_\perp)[M_{11}(\mathbf{k}_\perp)-1]-M_{12}^2(\mathbf{k}_\perp)}{\det[M(\mathbf{k}_\perp)]} J_1(k_\perp D). \tag{A8}$$

If we use Eqs. (A6) and (A8) in Eq. (A3), we have

$$A = \frac{Z_\alpha e}{\epsilon} \frac{1}{1 - D\int_0^\infty dk_\perp \frac{M_{11}(\mathbf{k}_\perp)[M_{11}(\mathbf{k}_\perp)-1]-M_{12}^2(\mathbf{k}_\perp)}{\det[M(\mathbf{k}_\perp)]} J_1(k_\perp D)}. \tag{A9}$$

This, when combined with Eq. (5), leads to

$$\psi_1(r_\perp) = \frac{Z_\alpha e\lambda}{\varepsilon} \frac{\int_0^\infty k_\perp dk_\perp \dfrac{M_{11}(\mathbf{k}_\perp)[M_{11}(\mathbf{k}_\perp)-1]-M_{12}^2(\mathbf{k}_\perp)}{\det[M(\mathbf{k}_\perp)]} J_0(k_\perp r_\perp)}{1 - D\int_0^\infty dk_\perp \dfrac{M_{11}(\mathbf{k}_\perp)[M_{11}(\mathbf{k}_\perp)-1]-M_{12}^2(\mathbf{k}_\perp)}{\det[M(\mathbf{k}_\perp)]} J_1(k_\perp D)}. \tag{A10}$$

Now $\psi_1(D,\zeta e) = \psi_1(r=D,e)|_{e\to e\zeta}$. Substituting $\psi(D,\zeta e)$ obtained this way into Eq. (7), we have

$$\frac{\mathcal{F}}{k_B T} = \frac{1}{2\pi}\left\{ \int_0^1 \frac{d\zeta}{\zeta} \frac{\int_0^\infty k_\perp dk_\perp \left[\dfrac{M_{11}(\mathbf{k}_\perp)[M_{11}(\mathbf{k}_\perp)-1]-M_{12}^2(\mathbf{k}_\perp)}{\det[M(\mathbf{k}_\perp)]}\right] J_0(k_\perp D)}{1 - D\int_0^\infty dk_\perp \left[\dfrac{M_{11}(\mathbf{k}_\perp)[M_{11}(\mathbf{k}_\perp)-1]-M_{12}^2(\mathbf{k}_\perp)}{\det[M(\mathbf{k}_\perp)]}\right] J_1(k_\perp D)} \right|_{e\to e\zeta} - \frac{1}{2D\lambda} \right\}. \tag{A11}$$

For later convenience, we rewrite the term in square brackets as

$$\left[\frac{M_{11}(\mathbf{k}_\perp)[M_{11}(\mathbf{k}_\perp)-1]-M_{12}^2(\mathbf{k}_\perp)}{\det[M(\mathbf{k}_\perp)]}\right] = \frac{1}{1+\lambda k_\perp} - \frac{M_{12}^2(\mathbf{k}_\perp)}{M_{11}(\mathbf{k}_\perp)\det[M(\mathbf{k}_\perp)]}. \tag{A12}$$

Note that the first term is h independent and that the coupling between the two plates enters through $M_{12}(\mathbf{k}_\perp)$—as expected, $M_{12}(\mathbf{k}_\perp)\to 0$ as $h\to\infty$. Equation (A11) becomes

$$\frac{\mathcal{F}}{k_B T} = \frac{1}{2\pi}\left\{ \int_0^1 \frac{d\zeta}{\zeta} \frac{\int_0^\infty k_\perp dk_\perp \left[\dfrac{1}{1+\lambda k_\perp} - \dfrac{M_{12}^2(\mathbf{k}_\perp)}{M_{11}(\mathbf{k}_\perp)\det[M(\mathbf{k}_\perp)]}\right] J_0(k_\perp D)}{1 - D\int_0^\infty dk_\perp \left[\dfrac{1}{1+\lambda k_\perp} - \dfrac{M_{12}^2(\mathbf{k}_\perp)}{M_{11}(\mathbf{k}_\perp)\det[M(\mathbf{k}_\perp)]}\right] J_1(k_\perp D)} \right|_{e\to e\zeta} - \frac{1}{2D\lambda} \right\}. \tag{A13}$$

Following Ref. [26], we find

$$\int_0^\infty k_\perp dk_\perp \frac{1}{1+\lambda k_\perp/\zeta^2} J_0(k_\perp D) = \frac{\zeta^2}{\lambda D}\tau_0\left(\frac{D}{\lambda}\zeta^2\right), \tag{A14}$$

$$1 - D\int_0^\infty dk_\perp \frac{1}{1+\lambda k_\perp/\zeta^2} J_1(k_\perp D) = -\frac{D\zeta^2}{\lambda}\tau_1\left(\frac{D}{\lambda}\zeta^2\right), \tag{A15}$$

where

$$\tau_n(x) = 1 - \frac{\pi x^{1-n}}{2}[H_n(x) - Y_n(x)], \tag{A16}$$

$H_n(x)$ is the Struve function, and $Y_n(x)$ is the Bessel function of the second kind. If we substitute Eqs. (A14) and (A15) into Eq. (A13), we obtain

$$\frac{\mathcal{F}}{k_B T} = \frac{1}{2\pi}\left\{ \int_0^1 \frac{d\zeta}{\zeta} \frac{\dfrac{\zeta^2}{\lambda D}\tau_0\left(\dfrac{D}{\lambda}\zeta^2\right) - \displaystyle\int_0^\infty k_\perp dk_\perp \frac{M_{12}^2(\mathbf{k}_\perp)}{M_{11}(\mathbf{k}_\perp)\det[M(\mathbf{k}_\perp)]} J_0(k_\perp D)}{-\dfrac{D\zeta^2}{\lambda}\tau_1\left(\dfrac{D}{\lambda}\zeta^2\right) + D\displaystyle\int_0^\infty dk_\perp \frac{M_{12}^2(\mathbf{k}_\perp)}{M_{11}(\mathbf{k}_\perp)\det[M(\mathbf{k}_\perp)]} J_1(k_\perp D)} - \frac{1}{2D\lambda} \right\}. \tag{A17}$$

From this we obtain, $\Delta\mathcal{F} = \mathcal{F}(h) - \mathcal{F}(h=\infty)$,

$$\frac{\Delta\mathcal{F}}{k_B T} = \frac{1}{2\pi}\int_0^1 \frac{d\zeta}{\zeta}\left\{ \frac{\dfrac{\zeta^2}{\lambda D}\tau_0\left(\dfrac{D}{\lambda}\zeta^2\right) - \displaystyle\int_0^\infty k_\perp dk_\perp \frac{M_{12}^2(\mathbf{k}_\perp)}{M_{11}(\mathbf{k}_\perp)\det[M(\mathbf{k}_\perp)]} J_0(k_\perp D)}{-\dfrac{D\zeta^2}{\lambda}\tau_1\left(\dfrac{D}{\lambda}\zeta^2\right) + D\displaystyle\int_0^\infty dk_\perp \frac{M_{12}^2(\mathbf{k}_\perp)}{M_{11}(\mathbf{k}_\perp)\det[M(\mathbf{k}_\perp)]} J_1(k_\perp D)} - \frac{\dfrac{\zeta^2}{\lambda D}\tau_0\left(\dfrac{D}{\lambda}\zeta^2\right)}{\left(-\dfrac{D\zeta^2}{\lambda}\right)\tau_1\left(\dfrac{D}{\lambda}\zeta^2\right)} \right\}. \tag{A18}$$

We find that, if $h \gg \lambda$,

$$\left| D\int_0^\infty dk_\perp \frac{M_{12}^2(\mathbf{k}_\perp)}{M_{11}(\mathbf{k}_\perp)\det[M(\mathbf{k}_\perp)]} J_1(k_\perp D) \right| \ll \left| \frac{D\zeta^2}{\lambda}\tau_1\left(\frac{D}{\lambda}\zeta^2\right) \right|.$$

This allows us to expand the denominator of the first term in Eq. (A18) in powers of the ratio

$$D\int_0^\infty dk_\perp \frac{M_{12}^2(\mathbf{k}_\perp)}{M_{11}(\mathbf{k}_\perp)\det[M(\mathbf{k}_\perp)]} J_1(k_\perp D) \Big/ \left[\frac{D\zeta^2}{\lambda}\tau_1\left(\frac{D}{\lambda}\zeta^2\right) \right].$$

To second order in the ratio, we find

$$\frac{\Delta\mathcal{F}}{k_BT} = \frac{1}{2\pi}\int_0^1 \frac{d\zeta}{\zeta} \left\{ \frac{\int_0^\infty k_\perp dk_\perp \frac{M_{12}^2(\mathbf{k}_\perp)}{M_{11}(\mathbf{k}_\perp)\det[M(\mathbf{k}_\perp)]} J_0(k_\perp D)}{\frac{D\zeta^2}{\lambda}\tau_1\left(\frac{D}{\lambda}\zeta^2\right)} - \frac{\frac{\zeta^2}{\lambda}\tau_0\left(\frac{D}{\lambda}\zeta^2\right)\int_0^\infty dk_\perp \frac{M_{12}^2(\mathbf{k}_\perp)}{M_{11}(\mathbf{k}_\perp)\det[M(\mathbf{k}_\perp)]} J_1(k_\perp D)}{\left[\frac{D\zeta^2}{\lambda}\tau_1\left(\frac{D}{\lambda}\zeta^2\right)\right]^2} \right\}. \tag{A19}$$

In the limit of $h \gg D$ and $h \gg \lambda$, the ζ integral in Eq. (A19) is mainly determined by $\zeta \sim \sqrt{\lambda/h}$, which is close to 0. In other words, the main contribution comes from $D\zeta^2/\lambda \sim D/h \ll 1$. This allows us to use the small-x expansions of the two functions $\tau_0(x)$ and $\tau_1(x)$:

$$\tau_0(x) \sim 1,$$

$$\tau_1(x) \sim -\frac{1}{x}.$$

Accordingly, Eq. (A19) becomes

$$\frac{\Delta\mathcal{F}}{k_BT} = \frac{1}{2\pi}\int_0^1 \frac{d\zeta}{\zeta} \left\{ -\int_0^\infty k_\perp dk_\perp \frac{M_{12}^2(\mathbf{k}_\perp)}{M_{11}(\mathbf{k}_\perp)\det[M(\mathbf{k}_\perp)]} J_0(k_\perp D) - \frac{\zeta^2}{\lambda}\int_0^\infty dk_\perp \frac{M_{12}^2(\mathbf{k}_\perp)}{M_{11}(\mathbf{k}_\perp)\det[M(\mathbf{k}_\perp)]} J_1(k_\perp D) \right\}. \tag{A20}$$

The ζ integral in this equation can be carried out without further approximations:

$$\frac{\Delta\mathcal{F}}{k_BT} = \frac{1}{8\pi}\int_0^\infty k_\perp dk_\perp \ln\left[1 - \frac{e^{-2hk_\perp}}{(1+\lambda k_\perp)^2}\right] J_0(k_\perp D) + \frac{1}{8\pi}\int_0^\infty dk_\perp \frac{k_\perp J_1(k_\perp D)}{1-e^{2hk_\perp}} \left\{ e^{2hk_\perp}\ln\left[1 - \frac{e^{-2hk_\perp}}{(1+\lambda k_\perp)^2}\right] + e^{hk_\perp}\ln\left[\frac{e^{hk_\perp}(1+\lambda k_\perp)-1}{e^{hk_\perp}(1+\lambda k_\perp)+1}\right] + 2\ln\left(1+\frac{1}{\lambda k_\perp}\right)\right\}. \tag{A21}$$

The free energy can now be expanded in powers of $1/h$. The lowest term scales as $1/h^2$ and the coefficient of this, a_2, can be obtained by multiplying $\Delta\mathcal{F}$ by h^2 and taking the limit of $h \to \infty$. To this end, we substitute $k_\perp = t/h$ in Eq. (A21); the first integral can then be calculated as follows:

$$\lim_{h\to\infty} h^2 \int_0^\infty k_\perp dk_\perp \ln\left[1 - \frac{e^{-2hk_\perp}}{(1+\lambda k_\perp)^2}\right] J_0(k_\perp D) = \lim_{h\to\infty}\int_0^\infty t\,dt \ln\left[1 - \frac{e^{-2t}}{(1+\lambda t/h)^2}\right] J_0\left(\frac{Dt}{h}\right) = \int_0^\infty t\,dt \ln(1-e^{-2t}) = -\frac{\zeta(3)}{4}. \tag{A22}$$

Similarly, we can get a_3, the coefficient of the next leading term, by taking $h \to \infty$ in $h^3(\Delta\mathcal{F} - a_2 h^{-2})$. We find, for $h \gg D$ and $h \gg \lambda$,

$$\frac{\Delta\mathcal{F}}{k_BT} \sim -\frac{\zeta(3)}{32\pi}\left[\frac{1}{h^2} - \frac{2\lambda}{h^3} + \frac{D}{h^3}\left(\ln\frac{h}{\lambda} - C\right)\right], \tag{A23}$$

where $\zeta(n)$ is the zeta function with $\zeta(3) \approx 1.202$ and $C = 1.707$. The first term is the universal power law, independent of surface charge densities and ionic sizes. The other two terms are the next leading corrections to $\Delta\mathcal{F}$. The third term arises from finite ionic sizes. It remains negative and thus makes the pressure more attactive as long as $h/\lambda \gg 1$. For $D/\lambda \gg 1$, this term dominates the second term. In the limit $h \gg D \gg \lambda$, Eq. (A23) reduces to Eq. (8) used in the main text.

[1] W. M. Gelbart *et al.*, Phys. Today **53** (9), 38 (2000).
[2] V. A. Bloomfield, Curr. Opin. Struct. Biol. **6**, 334 (1996).
[3] J. X. Tang, S. Wong, P. Tran, and P. Janmey, Ber. Bunsenges. Phys. Chem. **100**, 796 (1996).
[4] F. Oosawa, *Polyelectrolytes* (Marcěl Dekker, New York, 1971).
[5] B.-Y. Ha and A. J. Liu, in *Physical Chemistry of Polyelectrolytes*, edited by T. Radeva (Marcel Dekker, New York, 2001), p. 163.
[6] D. E. Leckband, C. A. Helm, and J. Israelachvili, Biochemistry **32**, 1127 (1993).
[7] G. S. Manning, J. Chem. Phys. **51**, 954 (1969).
[8] S. Marcělja, Biophys. J. **61**, 1117 (1992).
[9] P. Attard, R. Kjellander, D. J. Mitchell, and B. Jonsson, J. Chem. Phys. **89**, 1664 (1988).

[10] P. Attard, R. Kjellander, and D. J. Mitchell, Chem. Phys. Lett. **139**, 219 (1987); P. Attard, D. J. Mitchell, and B. W. Ninham, J. Chem. Phys. **88**, 4987 (1988).
[11] J. L. Barrat and J. F. Joanny, Adv. Chem. Phys. **94**, 1 (1996).
[12] P. A. Pincus and S. A. Safran, Europhys. Lett. **42**, 103 (1998).
[13] A. Sain and B.-Y. Ha, Physica A **320**, 67 (2003).
[14] D. B. Lukatsky and S. A. Safran, Europhys. Lett. **60**, 629 (2002).
[15] M. Kardar and R. Golestanian, Rev. Mod. Phys. **71**, 1233 (1999).
[16] I. Rouzina and V. A. Bloomfield, J. Phys. Chem. **100**, 9977 (1996).
[17] B.-Y. Ha and A. J. Liu, Phys. Rev. Lett. **79**, 1289 (1997).
[18] B. I. Shklovskii, Phys. Rev. Lett. **82**, 3268 (1999).
[19] J. J. Arenzon, J. F. Stilck, and Y. Levin, Eur. Phys. J. B **12**, 79 (1999).
[20] B.-Y. Ha, Phys. Rev. E **64**, 031507 (2001).
[21] A. W. C. Lau, P. Pincus, Dov Levine, and H. A. Fertig, Phys. Rev. E **63**, 051604 (2001).
[22] A. Moreira and R. R. Netz, Phys. Rev. Lett. **87**, 078301 (2001).
[23] A. Moreira and R. R. Netz, Eur. Phys. J. E **8**, 33 (2002).
[24] N. Gronbech-Jensen, R. J. Mashl, R. F. Bruinsma, and W. M. Gelbart, Phys. Rev. Lett. **78**, 2477 (1996).
[25] L. Guldbrand *et al.*, J. Chem. Phys. **80**, 2221 (1984).
[26] E. S. Velazquez and L. Blum, Physica A **244**, 453 (1997).
[27] D. A. Mcquarrie, *Statistical Mechanics* (Harper & Row, New York, 1971), Chap. 15.
[28] J. Israelachvili, *Intermolecular and Surface Forces*, 2nd ed. (Academic, San Diego, CA, 1992), Chap. 12.
[29] In a low-salt limit, this can be easily satisfied.
[30] R. N. Bracewell, *The Fourier Transform and Its Applications*, 3rd ed. (McGraw-Hill, Boston, 2000), p. 338, Table 13.2.